

# EVALUATION OF THERMAL BRIDGES IN VACUUM INSULATION PANEL ASSEMBLIES THROUGH STEADY-STATE TESTING IN A GUARDED HOT BOX

Brock Conley<sup>1</sup>, Cynthia A. Cruickshank<sup>1</sup>

<sup>1</sup>Carleton University, Ottawa Ontario, Canada

## ABSTRACT

Vacuum insulated panels (VIPs) offer high RSI-value insulation for building envelopes, where typical panels can be rated as high as RSI-4.16 per cm [R-60 per inch], however significant amounts of thermal bridging exist along their edges. A single layer of VIPs was evaluated by simulation and experiment using a steady-state guarded hot box. The thermal bridges were characterized, and an accurate reduction in RSI-value at points of interest, such as corners and edges, were found by using heat flux plates and embedded thermocouples. A second layer was implemented in three different configurations to study the edge thermal bridge effects and how different orientations affect performance. It was found that the non-homogenous VIP layers contained thermal bridges that caused a substantial RSI-value reduction, and can reach a 36% reduction in RSI-value when compared to the center of panel, and through using a different orientation of a second VIP layer can reduced the difference between maximum and minimum heat flux from 36% to 7%.

## INTRODUCTION

Vacuum insulation panels consist of a metallic envelope, generally aluminum, with a porous core material with a vacuum to eliminate conduction and convection through the center of panel [1], and potentially allowing VIPs to have a thermal resistance 10 times greater than traditional building insulating materials, per unit thickness [2]. The technology can increase the effective RSI-value of a dwelling thereby decreasing the required space heating and cooling. The benefits of using the panels include added insulation, but compared to traditional materials, it allows the wall thickness to remain comparable to typical dwellings and not reducing the useful area within the home. Previous studies on the thermal performance of the panels [3] used within this experimental have been conducted through in-situ and guarded hot box where a center of panel thermal resistance around  $2.5 \text{ m}^2\text{K/W}$ .

However, issues do exist and must be solved before widespread implementation can occur in buildings. The vacuum within the panel provides the high thermal resistance value, and while the metallic envelope provides a protective barrier, if it is punctured or vacuum is lost over time, the thermal resistance is reduced to an unknown value. Another factor is the non-homogenous nature of the panel, specifically how the thermal resistance at the center of the panel will vary from the value at the edge. This causes a variation in temperature at the warm surface of the panels. Therefore, when modelling the panels, using a center of panel value will result in an over estimated resistance value, while the edge value will result in an underestimated resistance value. This understanding is important as many of the energy performance standards require substantial modelling prior to being accredited.

Multiple studies have identified the need for further research and insight into VIPs and how they interact when installed within the building envelopes. P. Mukhopadhyaya of National Research Council of Canada [4] investigated the adoption of new envelope systems incorporating VIPs and barriers that exist before they can reach market, which include the buildability and energy performance assessment. They concluded that the further analysis of the edge effects that cause a significant loss of energy and reduce the overall envelope performance. Another study, performed by Natural Resources Canada, was about the design and modelling of the building envelope within a Net Zero Energy (NZE) home [5]. A main goal of the project was to achieve superior envelope performance while maintaining a wall thickness no greater than conventional homes. Their preliminary thermal and moisture transport modelling showed that the VIPs can act as an unintended vapour and moisture barrier, potentially causing moisture build up within the cavity if the VIP thermal resistance is sufficiently reduced.

The contributions presented in the paper include evaluating the thermal resistance difference between the center, edge and corner of a panel for a single VIP layer, how different orientations of the



specimen surface in the metering box) cannot vary by greater than  $\pm 0.25^\circ\text{C}$  and the heat flow from the metering chamber to guarded chamber does not exceed 1% of the heat input to the metering chamber.

The effective thermal resistance of the entire assembly can be found by using the specimen surface temperature difference in  $^\circ\text{C}$ , the metering chamber test area in  $\text{m}^2$ , the measurement time period in hours and the power input in Wh to the metering chamber by using Equation 1.

$$R = \frac{\Delta T * A * t}{q} \quad (1)$$

where  $\Delta T$  is the temperature difference between average hot and cold temperatures,  $A$  is the wall area in affected by the metering chamber,  $t$  is the elapsed time and  $q$  is the total heat input into the metering chamber.

In addition to the effective thermal resistance of the assemblies, the thermal resistances at points of interest, specifically where non-homogenous effects are anticipated, were desired. The temperature at each interface was measured and therefore a temperature difference at each layer was calculated. Therefore the thermal resistance can be determined within the envelope with the use of the embedded heat flux plates, which measure the heat flow in  $\text{W}/\text{m}^2$ , and temperature difference in  $^\circ\text{C}$  through Equation 2.

$$R = \frac{\Delta T}{q''} \quad (2)$$

where  $q''$  is the measured heat flux and  $\Delta T$  is the temperature difference across the layer.

The test specimen was built in order to isolate the thermal resistance effects of the VIP layer and embed the heat flux sensors to eliminate the effects of air movement, which can negatively impact the readings. A specimen was built by installing the plywood sheathing into the surround panel and adding building wrap to the cold side. The embedded thermocouples are placed on the building wrap and the VIPs are added using a pre-existing adhesive on the reverse side afterwards in a 4 x 3 layout. In order to find the difference in thermal resistance throughout the VIP on a single layer, embedded heat flux sensors were placed at a corner, edge and center of a VIP, and another panel was instrumented with thermocouples in a 5 x 6 evenly spaced grid. Using the heat flux and a

temperature difference at those points, a thermal resistance value was found at steady-state conditions. When the second layer of VIPs was introduced, three difference configurations were tested and heat flux readings at the same points of the single layer tests were taken.

In addition to the variation in thermal resistance value, a temperature variation throughout the VIP was found. By using the embedded thermocouples it was possible to create a heat map of a single VIP within Excel. By using the 5 x 6 grid of thermocouples embedded in the wall assembly, and linearly interpolating the temperature between these points, a heat map was created. To verify that the temperature trends, such as the edges and corners, are accurate, infrared thermal images were taken.

## EXPERIMENTAL WORK

In total, four steady-state experiments were performed to determine the thermal resistances for all points of interest. These included one test using a single layer of VIP between a 50.8 mm (2") of expanded polystyrene (EPS) on the cold side and 12.7 mm (0.5") plywood and three tests incorporating a second layer of VIPs using different configurations. Each test was performed at a different set of environmental conditions, but a temperature difference in excess of  $30^\circ\text{C}$  was achieved at steady-state for each situation. The temperature at each interface within the assembly, shown in Figure 2, will reach a point where the temperature change is very limited and steady-state is reached. The cycling on the climate surface is due to the cyclic nature of the cooling equipment. In Figure 2, the metering surface is the temperature of the specimen in the metering chamber, the air curtain is the air temperature 10 cm away from the surface, VIP PLY is the temperature between the plywood and VIP layer, EPS VIP is the temperature between the VIP layer and the first EPS board, EPS EPS is the temperature between the two EPS boards and climate surface is the specimen surface temperature in the climate chamber which is the surface of the second EPS board.

To achieve the goals of evaluating the difference in thermal resistance between the panel center, edge and corner as well as different configurations of the second layer instrumentation layout should be carefully considered, specifically heat

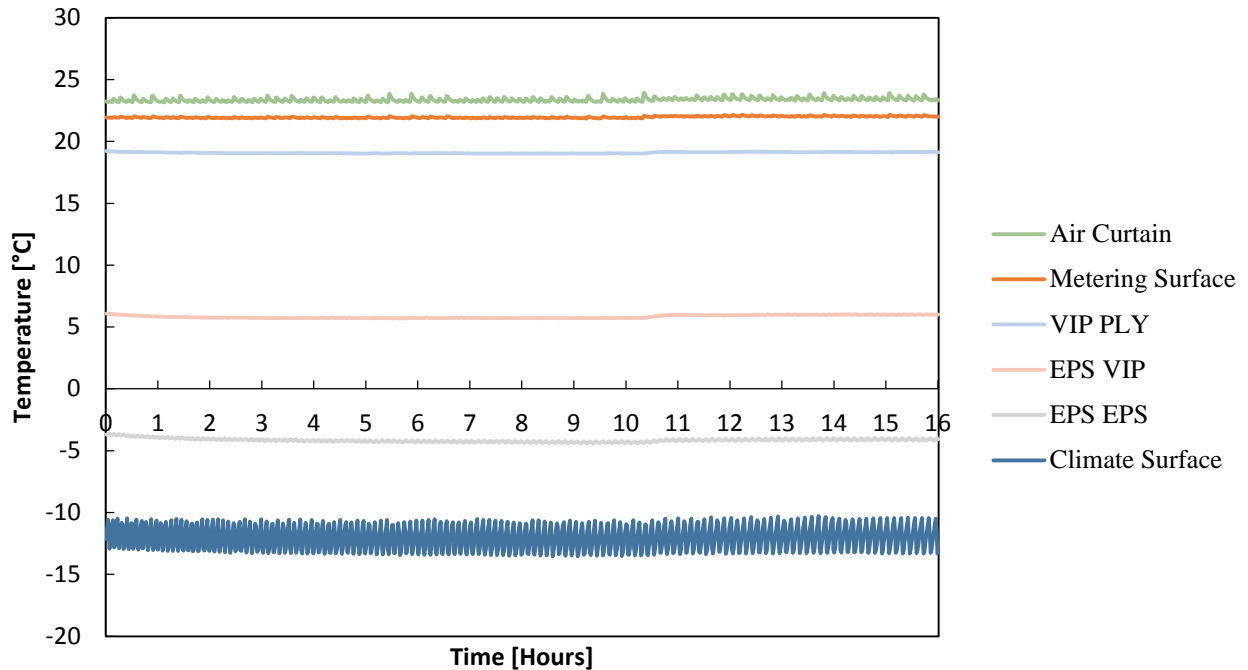


Figure 2: Steady-state temperature profile at each layer

flux plates and thermocouples. One VIP was heavily instrumented, as seen in Figure 3, in a grid pattern to obtain the temperature variation of one panel. The bubbles and numbers in the schematic indicate temperature sensors and locations labelled “HF” are the embedded heat flux plates. The exterior lines of the schematic indicate the walls of the surround panel, used to install and fix the specimen between the climate and metering chambers, and the outside of the VIP layer is 5.5” from the wall, on either side. The heat flux plates were placed at the center, edge and corner of the first layer of VIPs, and remained in the same position when testing the different orientations.

When installing the second layer of VIP to the wall assembly, it was possible to vary the configurations to change the temperature distributions and effective thermal resistance. Three different configurations for the second layer testing were chosen: center-center, center-edge and center-corner. The labelling of each configuration is based on where the panel center of the second layer is located with respect to the first layer. The initial layer was left unchanged throughout testing and was configured in a 4 by 3 VIP layout, also shown schematically as inner solid black lines in Figure 4, throughout testing. Therefore, in the center-center configuration, the panel center of the

second layer is located at the panel center of the first layer, and in the center-edge configuration, the panel center is located at the midpoint of the edge, and finally in the center-corner configuration, the panel center is located at a corner in the first layer. The panels used were all the same size, 457 mm by 558 mm (18” x 22”), same thermal properties and came from the same

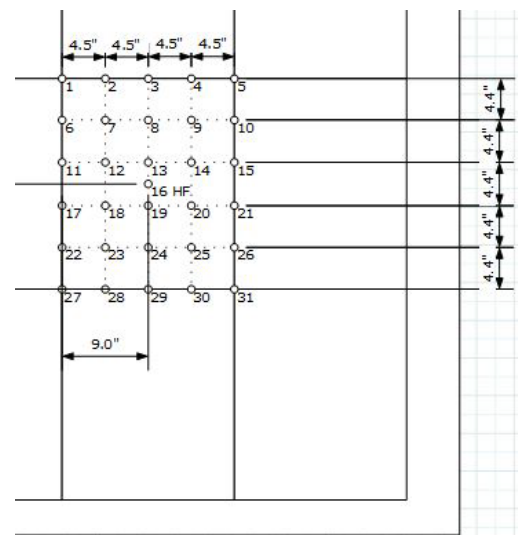


Figure 3: Embedded instrumentation layout for a single layer VIP

manufacturer. The schematics of tests including a second VIP layer and associated configurations can be found in Figure 4.

## RESULTS

The evaluation of the single VIP layer included finding the effective thermal resistance of the layer, the thermal resistance of center of panel, edge of panel and corner of panel and finally finding the temperature distribution on the warm side of the panel. During the test period, it was found that it required  $40.9 \text{ Wh} \pm 0.6 \text{ Wh}$  to maintain a temperature difference of  $34.0^\circ\text{C} \pm 0.6^\circ\text{C}$  across the entire wall assembly. Further, the heat flow through the metering chamber walls was found to be negligible based on the temperature measurements of the inside and outside walls of the metering chamber, their known thermal resistance and known area, therefore the heat flow through the assembly was equal to the heat input to the chamber. Using these values,

along with the known area of metered interface of  $1.83 \text{ m}^2$ , an effective RSI-value for the assembly was  $3.79 \text{ m}^2\text{K/W} \pm 0.2 \text{ m}^2\text{K/W}$ . The test conditions were added to Table 1, where the hot is the temperature measured on the assembly surface within the metering chamber, cold is the assembly surface temperature inside the climate chamber, heat input is the power into the metering chamber through the electric fans, and the eff RSI is the measured effective thermal resistance of the entire assembly.

Table 1: Conditions for the single VIP layer assembly

| Test Conditions                    |       |
|------------------------------------|-------|
| Cold [ $^\circ\text{C}$ ]          | -12.1 |
| Hot [ $^\circ\text{C}$ ]           | 22.0  |
| Heat Input [Wh]                    | 40.8  |
| Time [h]                           | 2.5   |
| Eff RSI [ $\text{m}^2\text{K/W}$ ] | 3.8   |

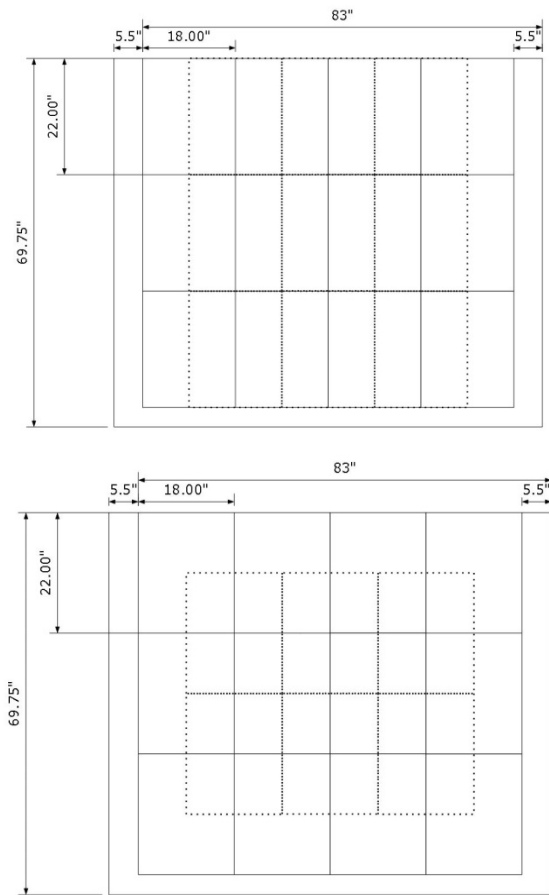


Figure 4: Schematic of Center-Edge (top) and Center-Corner (bottom) configurations

In addition to the overall thermal resistance of the VIP layer, the thermal resistance for the three main points of interest were found using the embedded heat flux plates and thermocouples. The grid of thermocouples was characterized either as center, an edge or a corner. It is summarized as 4 locations used to average the corner temperature {1, 5, 27, 31}, 14 used to average the edge temperature {2, 3, 4, 6, 10, 11, 15, 17, 21, 22, 26, 28, 29, 30} and the remaining 13 used to average the center temperature, where the numbers are represented as locations designated in Figure 3. The temperature difference is found by averaging three temperature measurements, located at the interface of EPS and VIP.

Thermal images were taken after steady-state was reached and five consecutive time periods had completed. The metering and guard chambers were removed from the experimental set-up and the images were captured. It is apparent in the photos shown in Figure 5 that a significant temperature gradient does exist along the VIP edges. In the photo, the outline of the VIP can be seen as blue representing the lower surface temperature, while the red represents the highest temperature and what can be characterized as the center of panel values. Even though the camera is reading the plywood surface temperature, the plywood has a very small thermal resistance and a thickness of 12.7 mm therefore the trend is representative of the

temperature distribution of the VIP PLY interface. It should be noted that the temperature color scales vary for each picture however the trends can still be observed.

The second layer of VIP was added in three different configurations for the purpose of finding the impact that each orientation has on the effective thermal resistance and how the heat flux changes within different orientations. The test conditions organized into Table 2 are the averages of 5 test periods after reaching steady-state through the ASTM C1363-11 [6] checks. The temperatures were measured at each interface within the assembly to graph the temperature profiles used for steady-state conditions and thermal resistance from the heat flux plates.

Table 2: Test Conditions for double VIP layer, all configurations

| Conditions                   | Center-Center | Center-Edge |
|------------------------------|---------------|-------------|
| Cold [°C]                    | -11.2         | -12.8       |
| Hot [°C]                     | 22.3          | 22.0        |
| Heat Input [Wh]              | 11.7          | 13.2        |
| Eff RSI [m <sup>2</sup> K/W] | 5.3           | 4.8         |
|                              | Center-Corner |             |
| Cold [°C]                    | -11.9         |             |
| Hot [°C]                     | 22.2          |             |
| Heat Input [Wh]              | 13.4          |             |
| Eff RSI [m <sup>2</sup> K/W] | 4.7           |             |

The embedded thermocouples were also used to facilitate the development of a heat map for a single VIP in Microsoft Excel. The heat map was developed to aid in illustrating the temperature distribution without using an infrared camera and required temperature measurements on the warm side of the VIP.

## DISCUSSION

From these results, both qualitative and quantitative, it can be seen that there is a large discrepancy between the heat fluxes through different sections of the panel, shown in Table 3. As expected, in the single layer test, the highest thermal resistance exists at the center, and then the edge and corner respectively. When the edge and corner values are compared to the center, the thermal resistance is

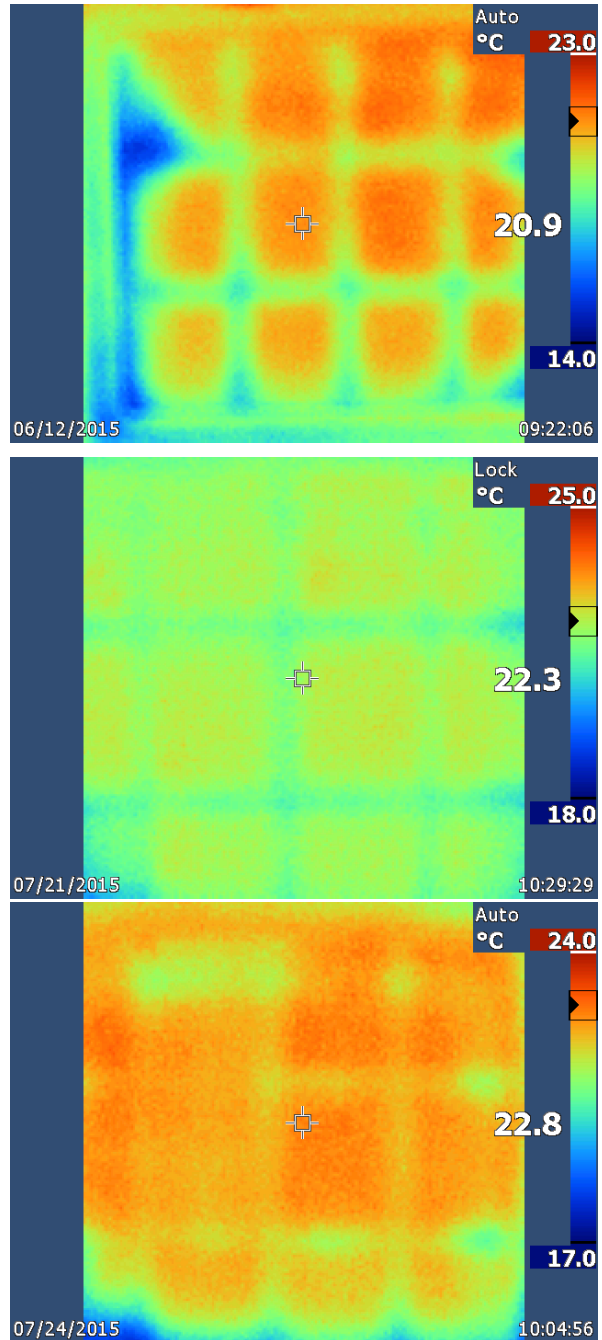


Figure 5: Infrared images for different configurations. From top to bottom: center-center, center-edge, center-corner

reduced by 32% and 36%, respectively. This is a substantial difference to take into account when attempting to model this layer as a homogenous insulation material. Another observation included comparing the thermal resistances to the panel rating from the manufacturer. While it should be noted the panels were not tested immediately after fabrication, or delivery from manufacturer, the center of panel thermal

resistance was 44% lower than the RSI-4.16 per cm VIP rating, and the difference was greater than 60% when compared to the edge and corner of the panels.

Table 3: Difference in heat flux for a single VIP

|                                      | Center | Edge | Corner |
|--------------------------------------|--------|------|--------|
| RSI Value [ $\text{m}^2\text{K/W}$ ] | 2.38   | 1.63 | 1.52   |
| % Reduction from Center              | -      | 32%  | 36%    |

With the infrared camera and the embedded temperature sensors, an Excel tool was developed to aid in visualizing the temperature distribution on the VIP. In Figure 6, a thermal image was taken of the VIP that was heavily instrumented with thermocouples, and an outline was added to distinguish where the VIP edges are approximately located and the heat map from Excel directly below. Each cell was used to represent a small area on the VIP, where the cells with white are the measured values and the black numbers are linearly interpolated between two control values. The Excel heat map has the ability to set the color scale manually, which is currently unavailable with these thermal images. Currently, many temperature values are required to produce an accurate visual representation of the temperature distributions, which is a limiting factor for using the tool, since these temperatures are not readily available at all times. However, through development and further testing of VIPs This tool can be also be used determine the point thermal resistances along the whole panel, which will aid in future modelling the non-homogenous thermal properties in steady-state heat transfer software.

The results from the second series of tests showed that the configuration of the panels can drastically change the temperature variations at the surface and the difference in heat flux through the assembly. As originally anticipated, the center-center configuration showed the same trends as the initial single layer test, such that there is a wide variation between the heat flux at the center compared to the edge and corners as well as the surface temperature. When the configuration was changed to center-edge, through the infrared images shown in Figure 5, the surface temperatures are becoming more homogenous, however variation still exists. This observation is also supported by the embedded heat flux readings since

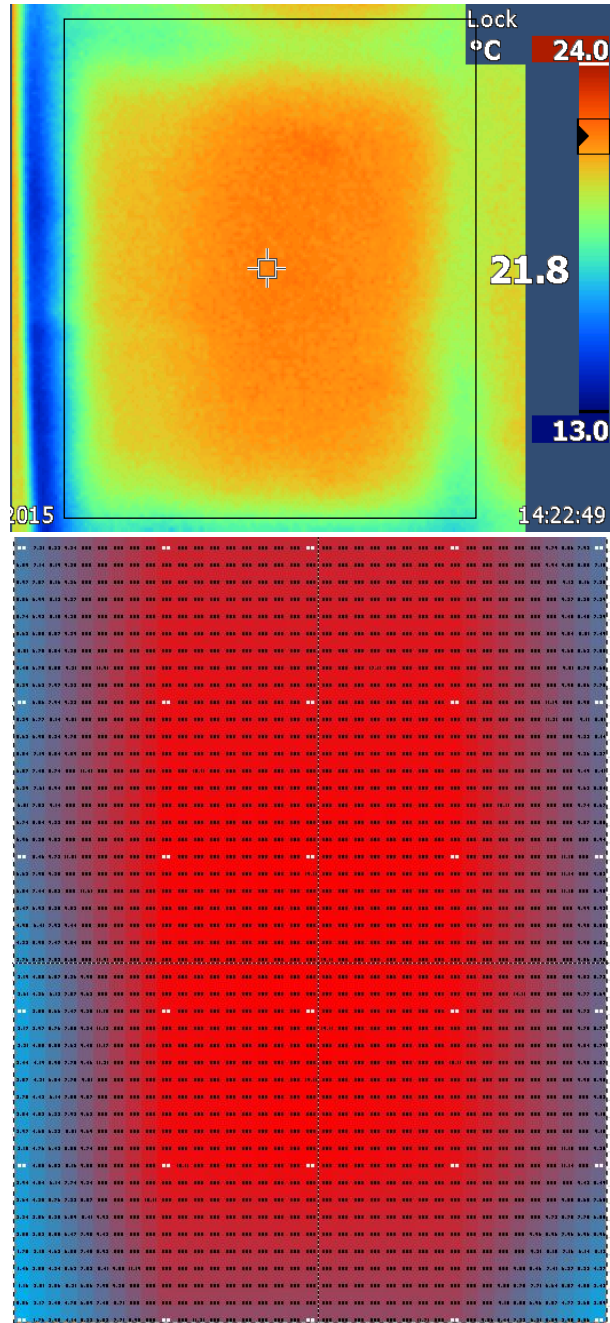


Figure 6: Infrared picture (top) and heat map in Excel (bottom) of a single VIP

their variance between the maximum and minimum have been reduced. Finally, the thermal images and the heat flux data indicated that the variation in the last configuration, center-corner, was minimal compared to the others. In Figure 7, the difference between the maximum and minimum heat flux measured by the embedded sensors, was graphed over the test period and an average of 36% for the center-center configuration, which has the most variations, and an

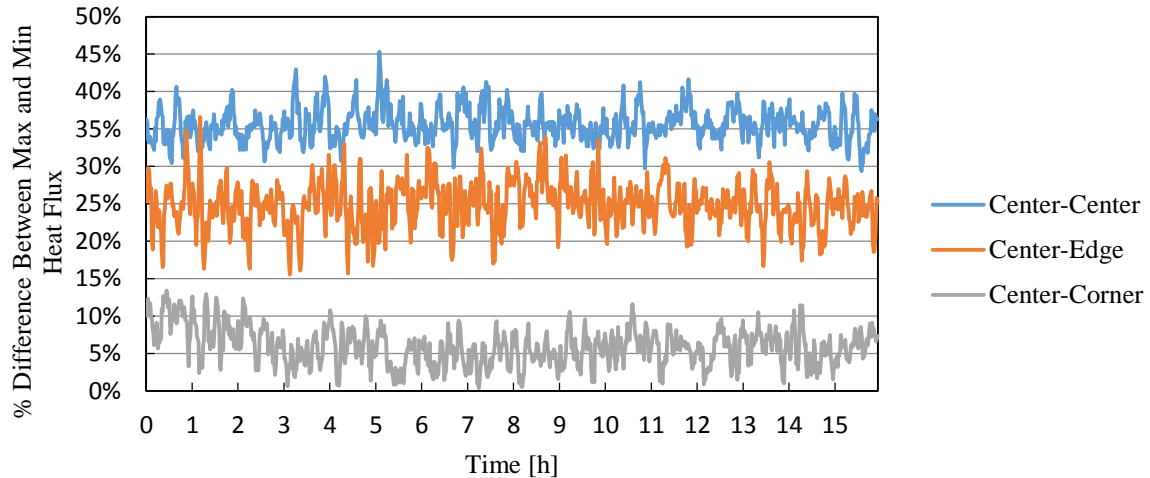


Figure 7: Difference between maximum and minimum heat flux over the test period

average of 7% for the center-corner configuration, which has the least variations. Overall, the difference in heat flux still exists, but it appears that the layer has the potential to be modelled as homogenous if the configuration is appropriate.

## CONCLUSIONS

The study was a thermal resistance evaluation of a single and double VIP layer with different configurations, including the point thermal resistance at key locations of interest. The results showed that at large reduction in RSI-value occurs between the center of panel and along the edges and corners, with a difference of 32% and 36% respectively. It also showed that when a second layer of VIPs are introduced, the orientation greatly affects the heat flux through the wall assembly since the difference between maximum and minimum heat flux through the assembly can be reduced from an average of 36% to 7%. Off-setting the panels such that the highest thermal resistance of one layer aligns with the lowest thermal resistance of the second layer impacts the surface temperature since the VIP outlines are not nearly as apparent in thermal imaging, however the effective thermal resistance remains minimally affected.

## FUTURE WORK

Future work will be conducted on determining an effective method at modelling these non-homogenous effects that VIP introduce into a wall assembly, specifically a method to create a single cross

section that will represent the multiple cross sections that exist within the assembly. As well, the Excel based heat map will be further developed to reduce the amount of data points required to produce an accurate representation of the temperature distribution, through further testing specific to the temperature gradient from the edge to the center.

## ACKNOWLEDGEMENTS

The authors would like to acknowledge the financial support of the Natural Science and Engineering Research Council (NSERC) of Canada.

## REFERENCES

- [1] R. Baetens, B. P. Jelle, J. V. Thue, M. J. Tenpierik, S. Grynning, S. Uvslokk and A. Gustavsen, "Vacuum insulation panels for building applications: A review and beyond," *Energy and Buildings*, no. 42, pp. 147-172, 2010.
- [2] P. Mukhopadhyaya, D. MacLean, J. Korn, D. van Reenen and S. Molleti, "Building application and thermal performance of vacuum insulation panels (VIPs) in Canadian subarctic climate," *Energy and Buildings*, no. 85, pp. 672-680, 2014.
- [3] C. Baldwin, C. A. Cruickshank, M. Schiedel and B. Conley, "Comparison of steady-state and in-situ testing of high thermal resistance walls incorporating vacuum insulation panels," in *6th International Building Physics Conference*, Turino,

2015.

- [4] P. Mukhopadhyaya, K. Kumaran, F. Ping and N. Normandin, "Use of vacuum insulation panel in building envelope construction: advantages and challenges," in *13 th Canadian Conference on Building Science and Technology*, Winnipeg, 2011.
- [5] A. Parekh and C. Mattock, "Incorporation of Vacuum Insulation Panels in a Wood Frame Net Zero Energy Home," *International Vacuum Insulation Symposium*, no. 10, pp. 46-50, 2011.
- [6] "Standard Test Method for Thermal Performance of Building Materials and Envelop Assesmbles by Means of a Hot Box Apparatus," ASTM International, West Conshohocken, PA, 2011.